Int. J. Appl. Ceram. Technol., 8 [6] 1289–1295 (2011)
DOI:10.1111/j.1744-7402.2010.02578.x

International Journal of
Applied Ceramic TECHNOLOGY
Ceramic Product Development and Commercialization

Influence of Residual Monomer on Cracking in Ceramics Fabricated by Stereolithography

Chang-Jun Bae* and John W. Halloran

Materials Science and Engineering, University of Michigan, Ann Arbor, Michigan 48109

The conventional build methods for polymeric stereolithography intentionally leave small regions of uncured monomer. We show that for ceramic stereolithography, these regions of uncured monomer are associated with macrocracking during heating. The cracking is caused by strains arising from the thermal polymerization of residual monomer while heating. Cracking can be avoided by changing the build style to eliminate the residual monomer.

Introduction

Solid freeform fabrication is the general name for an emerging technology in which sophisticated three-dimensional objects can be produced directly from a layer-by-layer process based on computer-aided design files. Stereolithography is a prominent technique among the solid freeform fabrication processes. Polymer objects from conventional stereolithography are built by selectively patterning a sequence of thin layers of a photosensitive liquid resin, using a scanning UV laser beam to photopolymerize the resin, thereby "writing" the design for each layer. After the sequence of many layers is complete, the uncured liquid resin is drained, leaving the solid polymer object with the desired design. Several groups have shown that the ceramic objects can be made using stereolithography, by replacing the resin with a photopolymerizable suspension of ceramic powder.[1–5] The resulting shaped object is a ceramic green body, consisting of ceramic powder in a polymer binder. To complete the ceramic process, the polymer is removed by thermal pyrolysis in a binder burnout heat treatment up to about 600°C. The binder-free object can then be sintered at higher temperature.

We have found that producing crack-free ceramics can depend on certain details of the laser curing

This work was supported by the Office of Naval Research under Grant N00421-06-1-0002.
*Baecj@mit.edu

technique, which this paper addresses. To describe this, it is necessary to consider the laser curing during stereolithography in more detail. The layers are built from a pattern of lines. The scanning laser beam polymerizes a thin line of material, with a line width L_w. An area is polymerized by a sequence of closely spaced lines, or vectors. The laser scanning is conducted according to a build style, which controls X and Y directions of the UV laser. Monomers have lower density than their polymers, and hence polymerization is accompanied by polymerization shrinkage. If a build style is inappropriate, defects such as delamination, distortion, and bending in the green body can be induced due to the polymerization shrinkage. Conventional unfilled resins are commonly use a staggered-weave build style[6] to avoid the distortion from internal stress developed from polymerization shrinkage during part building. Each layer is cured by first defining the perimeter of the cured area by drawing "border vectors." Next, the inside of the perimeter is cured with "fill vectors" by "hatching." Conventional build styles intentionally leave a small uncured gap between the border vectors and the fill vectors. This gap is known as the "end retract." If the spacing between lines, or the "hatch spacing," is larger than the line width of the fill vectors, there may be uncured residual monomer as thin lines between the fill vectors. The hatch spacing and end retract are parameters in the "staggered-weave" build style, which is commonly used for stereolithography.

This staggered-weave build style was developed to reduce internal stress due to polymerization shrinkage,[6] which improved accuracy for polymeric materials. Figure 1a illustrates staggered hatch style, which is a method to avoid weak spots and a tendency to develop long cracks directly. The fill vectors on the n-th layer are offset by exactly half the regular hatch spacing ($h_s/2$), relative to fill vectors on the $(n-1)$-th layer. The advantage of this hatch is to intentionally offset the fill vectors on successive layers to reduce stress concentrations along the relatively weaker regions between fill vectors. The end-retracted hatch style in Fig. 1b is intended to avoid internal shrinkage strains border vectors. One end of each hatch vector is attached to one of the borders, but does not connect to the opposite border. Hatch vectors in X or Y direction are only attached at one border so that the first pass hatch vectors do not generate any reactive forces resulting from shrinkage forces to be exerted on the borders. Note that the end retract leaves a small volume of residual liquid monomer.

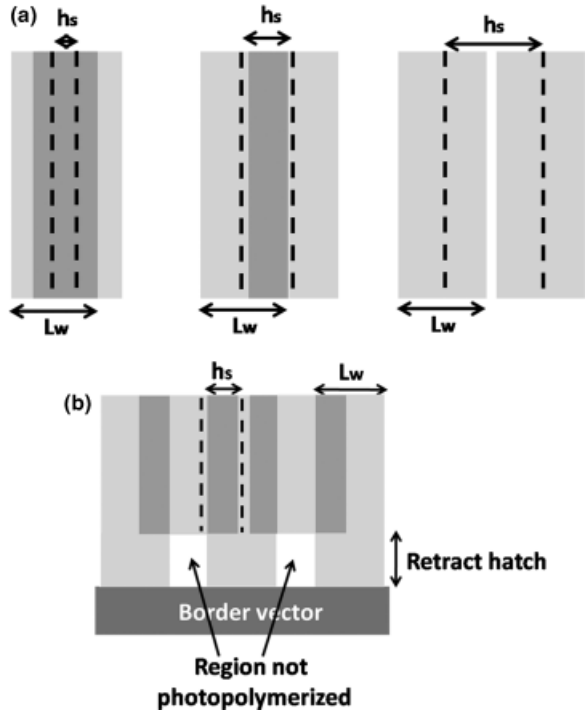

Fig. 1. (a) Schematic illustrating hatch spacing for two fill vectors with 90 μm line with and 25 μm hatch spacing (left), 50 μm hatch spacing (center), and 100 μm hatch spacing (right); (b) illustration of a series of border vectors with adjacent 90 μm fill vectors with 50 μm hatch spacing and 100 μm end retraction. Note the region of monomer that is not photopolymerized.

In this paper, we show that sintered ceramics built with a build style with staggered and end-retraction hatches display cracks. We associate these cracks with uncured monomer and photoinitiator located at the end-retracted hatch. The residual monomer and photoinitiator are detected using gas chromatography. We show that a build style with no end retraction can produce sintered ceramics with no cracks.

Experimental Procedure

Ceramic Stereolithography Technique

A photopolymerizable suspension is prepared from ceramic powder, a photoreactive monomer solution, and photoinitiator were prepared as described in detail elsewhere.[7] The monomer mixture was a blend of 90 wt% 1,6-hexanediol diacrylate (HDDA, SR238)

and 10 wt% ethoxylated pentaerythritol tetraacrylate (EPTA, SR494). Both monomers were used as received from the manufacturer (Sartomer, Exton, PA). The photoinitiator was 1-hydroxy cyclohexyl phenyl ketone (Irgacure 184, Ciba Specialty Chemicals, Tarrytown, NY). The ceramic powder was a refractory fused silica (SiO_2, PCC Airfoils, Sanford, NC) with a median size d_{50} of 12 μm. The particle sizes ranged from d_{10} of 3 μm to d_{90} of 66 μm. The colloidal dispersant was a quaternary amine (VariquatCC-59, Goldschmidt, Essen, Germany) that was added in an amount equal to 3% of the weight of the SiO_2 powder. The ceramic solid loading was 60 vol%. The photoinitiator, at a concentration of 2 wt% with respect to the monomer, was added to a 60 vol% suspension. Bubbles were removed from the completed suspension by vacuum deairing.

Fabrication was performed with a commercial stereolithography apparatus (SLA-250/40, 3D Systems, Valencia, CA) with a 355 nm quasicontinuous wave UV laser (Xcyte CY-SM60, JDS Uniphase, Milpatis, CA). The beam diameter was 125 μm and the output power was 40 mW. The resin sensitivity D_p (depth where the laser intensity is reduced by 1/e) was 805 ± 48 μm and the critical energy dose was 15 ± 1.29 mJ/cm^2. The layer thickness was 100 μm. For these conditions, the calculated line width was 90 μm. An investment casting mold model,[8] about 100 mm tall and up to 39 mm wide with 1407 layers, was built with these conditions using a standard hatch spacing (h_s) of 52 μm and end retraction of 200 μm. A series of small cube specimens were built with hatch spacing varying from 25 to 100 μm and end retractions varying from 0 to 200 μm. The binder burnout was conducted by slow heating in air up to 600°C, followed by sintering at 1300°C for 30 min. The binder burnout cycle had a sequence of steps: 5°C/min to 335°C, 1°C/min to 415°C, 3°C/min to 480°C, and 2°C/min to 600°C. Sintering at 1300°C causes about 10% of the fused silica to devitrify to cristobalite.[8]

Thermogravimetric Analysis (TGA) and Differential Scanning Calorimeter (DSC)

TGA was used to characterize the pyrolysis of the polyacrylate binder in the green ceramics. Samples of 5–20 mg placed in alumina pans were examined in a simultaneous TGA–DTA instrument (SDT2660, TA Instruments, New Castle, DE) with a heating rate of 5°C/min to 600°C in air. Polymerization of the residual monomer was examined using differential scanning calorimeter (DSC) at a heating rate of 5°C/min, using a Thermal Analyst model 2100 system equipped with a model 2910 MDSC cell (TA Instruments). The sample compartment was continuously purged with dry nitrogen at 50 mL/min.

Gas Chromatography/Mass Spectrometry (GC/MS)

The nature of the residual monomer was characterized by GC and MS. A five-layer sample, 1 mm thick, was built as a green sheet with an end-retracted hatch of 200 μm. After building, the uncured suspension adhering to the surface was thoroughly removed by rinsing in isopropanol. The cleaned sample was crushed to a powder, and was submerged in dichloromethane (CH_4Cl_2) for 4 h to extract the residual monomer formed inside the sample at the end-retracted hatch. The extract was analyzed on a Finnigan Trace GC/MS, equipped with a Supelco SLB-5 column, using helium at 1 mL/min as the carrier gas. The injector temperature was 200°C, set up for a splitless injection. The oven temperature was held at 30°C for 3 min, and then heated to 275°C at 20°/min. The mass range was set from m/z (mass-to-charge ratio) 35 to m/z 400, with electron energy of 70 eV. Identification of the components was performed by comparison of the mass spectra with ones found in the Wiley NBS library.

Results and Discussion

Binder Removal

TGA was applied to identify temperature regions of rapid mass loss of the green body of ceramic mold. Figure 2 represents the weight loss and temperature difference as a function of temperature for constant heating rate of 5°C/min. All the organic binders are removed below 600°C in air. There are four main mass removal events, the first of which occurs from 200° to 335°C removing 4 wt% of material, the second exothermic event from 335° to 415°C removing 21 wt% of material, the third exothermic event from 415° to 480°C removing 3 wt% of material, and the final event from 480° to 600°C removing the final 5 wt%. The exothermic events of the process demonstrate that the degradation involves oxidation reaction.

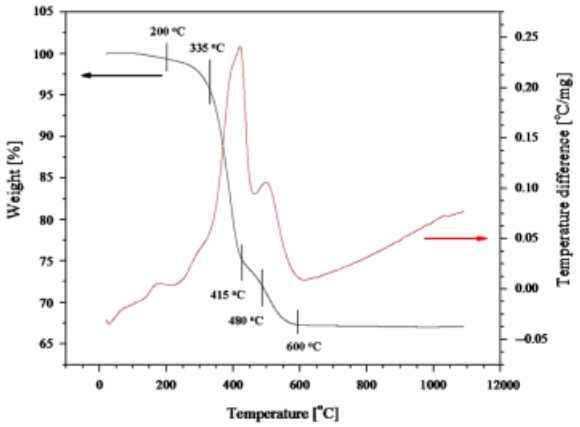

Fig. 2. Thermogravimetric analysis at 5°C/min of pyrolysis of polyacrylate in 60 vol% silica built by ceramic stereolithography showing mass loss accompanied by exothermic reaction.

Cracks Generated During Binder Removal from the Ceramic-Filled Green Body

The sintered ceramic mold model suffered prominent horizontal and vertical cracks, visible in Fig. 3. Horizontal cracks might be expected due to delamination between the layers. But these horizontal cracks are not simple delaminations. Rather, the horizontal cracks have frequent vertical jogs with jog displacements much larger than the 0.1 mm layer thickness. The vertical cracks are obviously not associated with the layered fabrication. The large crack-opening displacement, and close examination of the crack surface, suggests that these cracks were already open at high temperature, and are not likely to be associated with stresses during cooling or because of the ~250°C β–α cristobalite transformation during cooling. This part was examined after the sintering at 1300°C, and hence it was not clear if the cracks occurred (a) before significant weight loss, caused by phenomena unrelated to pyrolysis; (b) during the mass loss during pyrolysis, caused by phenomena associated with the burnout reactions and reaction product transport; or (c) during sintering, due to phenomena related to densification or cristobalite transformation. To discover the origin of the cracking, simple cube-shaped green specimens were used to determine the temperature at which cracks initiate during heating. Like the mold model, these cubes were with a hatch spacing of 57 μm and an end retraction of 200 μm. The specimens were inspected at regular temperature increments between 20 and 600°C to seek the temperature where the damage could be first noticed. It appeared that the damage began before binder mass loss, or perhaps at the early stages of the process, and then became more severe during subsequent binder removal. No cracks were detected until they were heated below about 200°C. Figure 4a is a photograph of a cube specimen after heating to 240°C, before significant amount of mass has been lost due to binder burnout, suggesting that the cracks do not directly result from binder burnout. Two horizontal cracks are visible. Heating to higher temperature caused an increasingly severe cracking. Figure 4b shows extensive branching cracks, both horizontal and vertical, in a cube heated to 400°C. This is about 60% through the binder burnout process.

Cracking is obviously a response to mechanical strains. If the damage originated before significant binder burnout, the mechanical strains are probably not related to the pyrolysis reaction. Another hypothesis is that the strains were due to polymerization of the

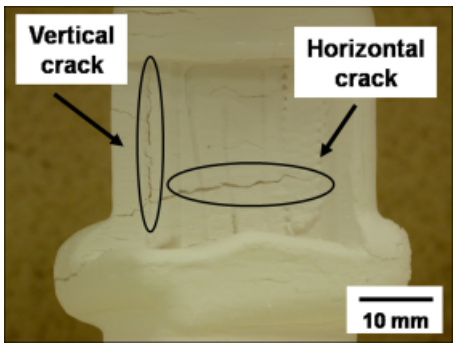

Fig. 3. Vertical and horizontal cracks of sintered ceramic mold fabricated by ceramic stereolithography. The layering direction is horizontal and build direction is vertical.

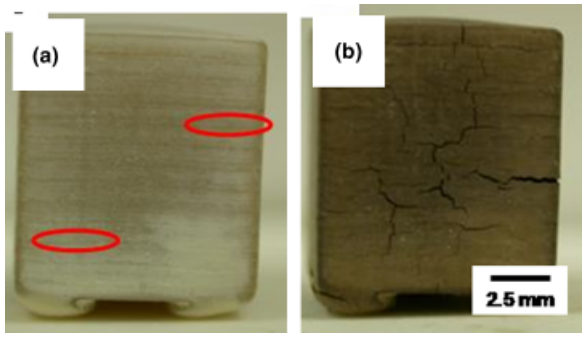

Fig. 4. Vertical and horizontal cracks detected in the green body built with hatch spacing of 57 μm and end retract of 200 μm heated to (a) 240°C and (b) 400°C.

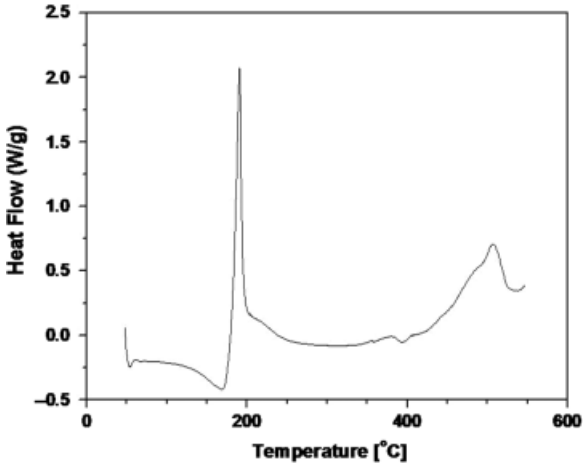

Fig. 5. Differential scanning calorimetry of 1,6-hexanediol diacrylate-EPETA monomer with ketone photoinitiatior. Exothermic heat flow around 200°C represents thermal polymerization induced by thermal decomposition of the photoinitiator.

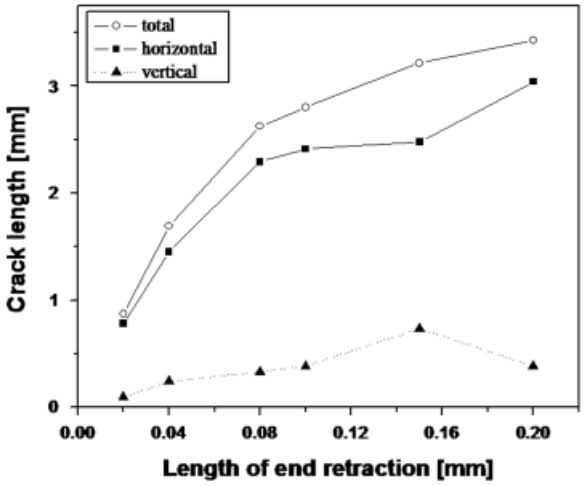

Fig. 7. Crack length as a function of length of end retraction.

residual monomer. The end-retract regions have, by design, small regions of unreacted monomer and photoinitiator. If the photoinitiator is thermally decomposed during heating, the resulting free radicals might cause the polymerization of the residual monomer. The subsequent polymerization shrinkage might be the origin of the mechanical strains that cause cracking.

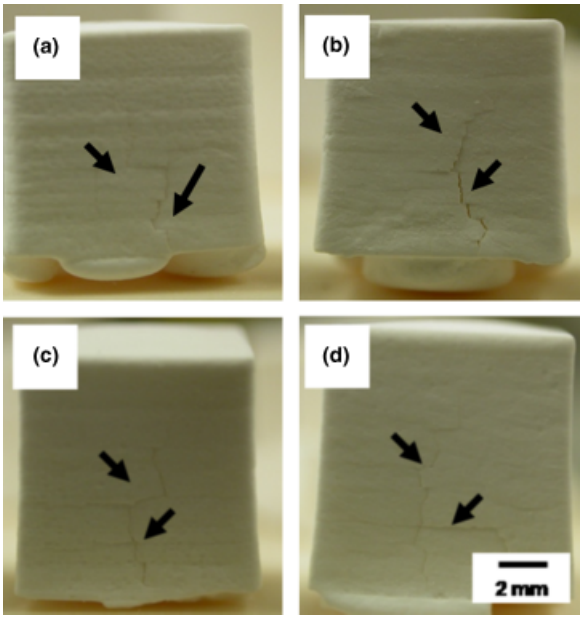

Fig. 6. Cracks generated in the whole regions for sintered cubes built with 200 μm of end retract and varying hatching space (h_s); (a) $h_s = 25$ μm, (b) $h_s = 50$ μm, (c) $h_s = 80$ μm, and (d) $h_s = 100$ μm.

Differential scanning calorimeter (DSC) was used to determine if the monomer could be in fact polymerized during heating. Figure 5 is a DSC scan for the HDDA–EPETA monomer mixture with the hydroxyketone photoinitiator before photopolymerization. Thermal decomposition of the 1-hydroxycyclohexyl phenylketone occurs as an endothermic event around 170°C, indicating the thermal decomposition of the photoinitiator to form free radicals. A large exothermic effect between 180 and 200°C is from the exothermic polymerization of the acrylates by the free radicals. Thus, as expected, the ketone photoinitiator serves as a thermal initiator if heated to ~200°C.

A series of experiments were conducted to systematically vary the hatch spacing and end-retract hatch. A series of cubes were fabricated with the same 200 μm end retract, but with hatch spacing varying from 25 to 100 μm. Because the line width from the laser scanning was ~90 μm, this means that the shorter hatch spacings had significant overlap of the fill vectors, and thus there should be little uncured monomer between the fill vectors, while the larger hatch spacings might have some residual monomer between the fill vectors. Figure 1a illustrates this schematically for three different hatch spacings. Figure 6 shows the variable-hatch spacing series of cubes after sintering at 1300°C. All the specimens display vertical and horizontal cracks, regardless

of the hatch spacing. This suggests that hatch spacing is not a decisive cause of cracking.

A second series of experiments were conducted where the end retract was varied. Figure 1b illustrates this, showing the region between the border vectors and the fill vectors for a particular set of lines width, hatch spacing, and end retract. Notice that end retraction leaves a small region that is not photopolymerized.

The extent of cracking was quantified by measuring the total length of all vertical and horizontal cracks visible on each specimen of sintered cubes. These are expressed as a crack length versus the length of the end retraction used in the build style. Figure 7 shows the length of horizontal cracks running in the layering direction, vertical cracks running against the layering direction, and their sum. The extent of cracking increases drastically with the length of the end retraction. The postsintering crack length is zero when the end retraction is zero, i.e. there are no detected cracks. Figure 8 shows a series of cubes built with zero end retract, and variable hatch spacing, after sintering. No cracks are apparent. Apparently, removing the end retract has eliminated cracking.

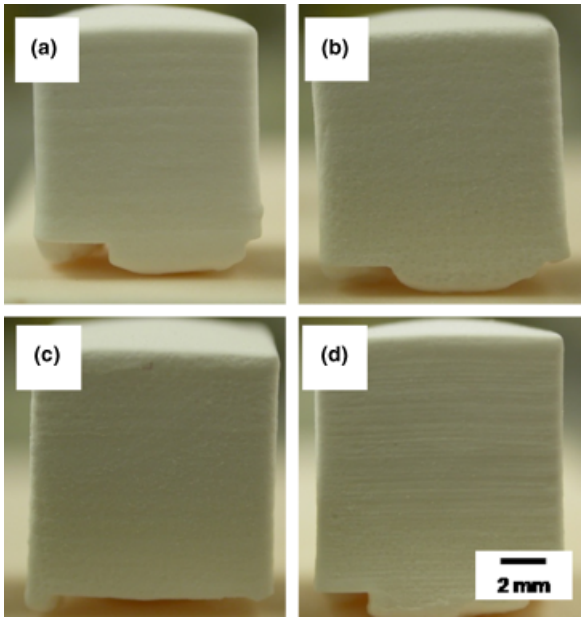

Fig. 8. Crack-free sintered cubes built with zero end retraction and variable hatch spacing: (a) $h_s = 25$ μm, (b) $h_s = 50$ μm, (c) $h_s = 80$ μm, and (d) $h_s = 100$ μm.

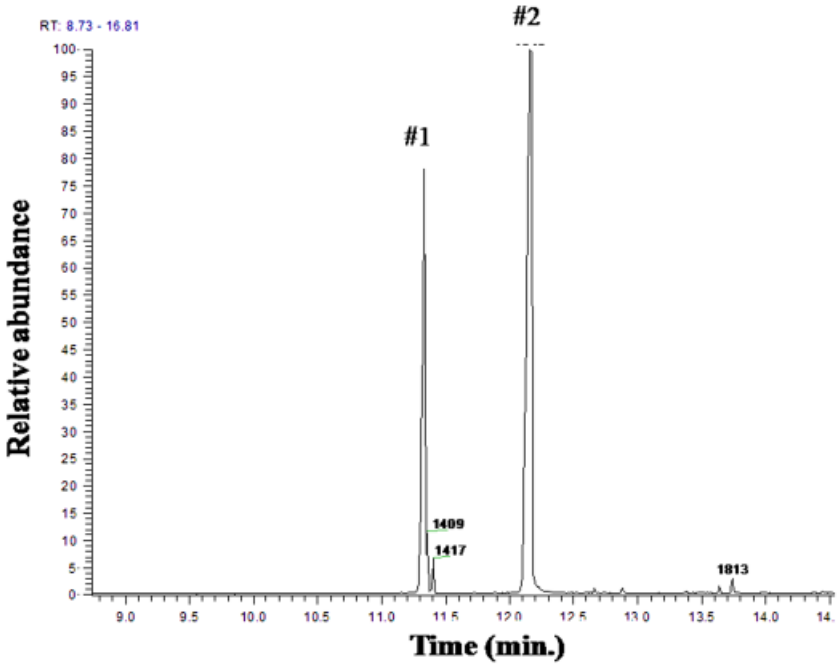

Fig. 9. Gas chromatography/mass spectrometric chromatogram of species extracted from photopolymerized silica–polyacrylate green sheet built with 200 mm end retraction. Peak #1 is from hexane diol diacrylate (HDDA) residual monomer and peak #2 is from Irgacure 184 photoiniator.

Residual monomer and residual photoinitiator can be detected in specimens built with 200 μm end retraction. Figure 9 shows two prominent peaks in a chromatograph of a material extracted from the green body with dicholoramethane. The mass spectra from the peak labeled #1 was identified as 2-propanoic acid, 1,6 hexane diyl ester (i.e., HDDA) and hence is from the residual monomer remaining after photopolymerization. Peak #2 was identified as Irgacure 184, and hence it is residual ketone photoinitiator. The detection of residual HDDA and residual ketone initiator after photopolymerization, combined with the DSC results of showing that the Irgacure 184 acts as a thermal initiator, supports the idea that residual monomer can polymerize during heating below the binder pyrolysis temperatures. We suggest that polymerization shrinkage provides the mechanical strain that results in the cracking observed in parts built with ceramic stereolithography using a build style with end retraction.

Conclusions

Ceramic bodies built by ceramic stereolithography from 60 vol% silica in acrylate monomers using a build style with end retraction have horizontal cracks along the layer direction and vertical cracks normal to the layering direction. The extent of cracking is not sensitive to hatch spacing of the fill vectors, but sensitive to end retraction between the fill vectors and the border vectors. Building with zero end retraction eliminates these cracks.

Cracking is observed around 200°C, before the beginning of significant mass loss during pyrolysis of the polyacylate binder in air, and hence the cracking is not caused by mass transport during pyrolysis. Residual monomer and residual photoinitiator can be detected in objects built with end retraction. The photoinitiator can behave as a thermal initiator and cause polymerization of the monomer at around 200°C, as detected by DSC. The cause of the cracking could be polymerization shrinkage due to the thermally induced polymerization of residual monomer that was not photopolymerized in the end-retraction region. Stereolithography build styles appropriate for polymeric materials may need to be modified for ceramic stereolithography.

Acknowledgement

This study was conducted as part of a collaboration with Mr. Wil Baker of Honeywell and PCC Airfoils, PLC.

References

1. J. W. Halloran, C.-J. Bae, C. Torres-Garibay, V. Tomeckova, S. Das, and W. Baker, "Manufacture of Complex Ceramics by Photopolymerization," *Global Roadmap for Ceramics—ICC2 Proceedings. The Proceedings of the 2nd International Congress on Ceramics, Verona, Italy, June 29–July 4, 2008. ISBN 978-88-8080-084-2*. eds., A. Bellosi, and B. G. Nicola. Agenzia Polo Ceramico S.C. A.r.l., Faenza, Italy, 369–378, 2008.
2. T. Chartier, C. Chaput, F. Doreau, and M. Loiseu, "Stereolithography of Structural Complex Ceramic Parts," *J. Mater. Sci.*, 37 [15] 3141–3147 (2002).
3. M. L. Griffith and J. W. Halloran, "Freeform Fabrication of Ceramics Via Stereolithography," *J. Am. Ceram. Soc.*, 79 [10] 2601–2608 (1996).
4. W. Zhou, D. Li, and H. Wang, "A Novel Aqueous Suspension for Ceramic Stereolithography," *Rapid Prototyping J.*, 16 [1] 29–35 (2010).
5. C. Exposito Corcione, A. Greco, F. Mongagna, A. Liccuiulli, and A. Maffezzoli, "Silica Moulds built by Stereolithography," *J. Mater. Sci.*, 40 [18] 4899–4904 (2005).
6. P. F. Jacobs, *Rapid Prototyping & Manufacturing—Fundamentals of Stereolithography*, SME, La Crescenta, California, 397–450, 1992.
7. C. -J. Bae, "Integrally Cored Ceramic Mold Fabricated by Ceramic Stereolithography," Ph.D. Dissertation, University of Michigan, 2008.
8. C. -J. Bae and J. W. Halloran, "Integrally Cored Ceramic Mold Fabricated by Ceramic Stereolithography," *Int. J. Appl. Ceram. Technol.*, (2010) in press.